Nonlinear dependence on Na^+ ions for the binding dynamics of cucurbit[6]uril with *trans*-1-methyl-4-(4-hydroxystyryl)pyridinium cation

Tang, H., Thomas, S. S., Wolf, L., Natarajan, P., Ko, Y. H., Wilson, J., . . . Bohne, C.

2020

Nonlinear Dependence on Na^+ Ions for the Binding Dynamics of Cucurbit[6]uril with *trans*-1-Methyl-4-(4-hydroxystyryl)pyridinium Cation

Hao Tang,[†,#] Suma S. Thomas,[†] Luise Wolf,[†] Palani Natarajan,[†,&] Young Ho Ko,[‡] James Wilson,[,§] Kimoon Kim,*[,‡,¶] and Cornelia Bohne*[,†]*

[†] Department of Chemistry and Centre for Advanced Materials and Related Technologies (CAMTEC), University of Victoria, PO Box 1700 STN CSC, Victoria, BC V8W 2Y2, Canada

[‡] Center for Self-assembly and Complexity (CSC), Institute for Basic Science (IBS), Pohang 37673, Republic of Korea

[¶] Department of Chemistry, Pohang University of Science and Technology (POSTECH), Pohang 37673, Republic of Korea

[§] Department of Chemistry, University of Miami, 1301 Memorial Drive, Coral Gables, FL 33124, United States

ABSTRACT

The binding dynamics of the *trans*-1-methyl-4-(4-hydroxystyryl)pyridinium cation (HSP^+) to cucurbit[6]uril (CB[6]) in the presence of Na^+ cations was studied to establish the effect of the relative concentrations of the system's components (HSP^+, CB[6], and Na^+) on these dynamics. The formation of the HSP^+@CB[6] complex was temporally uncoupled from the photoisomerization of *trans*-HSP^+, while a nonlinear effect of the Na^+ cation concentration on the HSP^+@CB[6] dynamics was observed. This nonlinearity is a consequence of Na^+ having the opposite effect on the association and dissociation rate constants for the HSP^+@CB[6] complex, creating a conceptual framework for using such nonlinearities to control multistep reactions in cucurbit[*n*]uril chemistry.

INTRODUCTION

Cucurbit[*n*]urils (CB[n]s) are versatile macrocycles that, as hosts, bind hydrophobic guests with positive charges,[1-4] leading to changes in the guest's chemical properties, such as changes in pK_a values[5-9] and shifts in redox potentials.[10-11] The broad range for the equilibrium constants of guest–CB[*n*] complexes (10^2–10^{17})[1-3, 12] makes CB[*n*]s suitable for studies of systems where competitive pathways for guest binding are desirable. Examples include studies of self-sorting systems,[13-17] applications for drug delivery[18-22] including pretargeting strategies for spatial control of drug release,[23] and uses in signaling cascades,[24] tandem enzymatic assays,[25-26] relay switch design,[27] and the dissolution of gel wound dressings.[28] A different type of competition in guest–CB[*n*] chemistry is the binding of metal cations to the carbonyl groups located at the portals of CB[*n*] cavities.[3, 29-30] This metal binding has been used to control the concentration of free CB[*n*][3, 29-30] or

the stoichiometry of guest–CB[*n*] complexes.[31] Metal binding has also been shown to switch the CB[*n*] binding mechanism for a ditopic guest.[32]

CB[*n*]s are used to alter chemical reactivity and are applied in particular for catalysis.[4, 12, 33-37] Understanding how CB[*n*] complexation affects coupled or sequential reactions will provide mechanistic information to help design and control the reactivity of systems using a supramolecular approach. In this respect, we chose to study a photoisomerization reaction that could be initiated on demand and the binding of one of the isomers to CB[6].

As the guest, the 1-methyl-4-(4-hydroxystyryl)pyridinium cation (HSP^+) was used. The key feature for the photoisomerism of this molecule is that protonated HSP^+ undergoes photochemical *trans*-to-*cis* and *cis*-to-*trans* isomerizations, whereas deprotonated *cis*-HSP is thermally unstable and reverts readily to *trans*-HSP (Scheme 1).[38] This property allowed for the design of kinetic experiments that were initiated by having only deprotonated *trans*-HSP present in solution at the start of the experiment. This design enabled the determination of the time domains for the guest–CB[6] binding dynamics and the photoisomerization reaction, and established a conceptual framework enabling the future design of orthogonal controls for the reactivity of coupled reactions modulated by the concentration of metal cations.

Scheme 1. Structure of cucurbit[6]uril (CB[6]), and protonation and isomerization of the 1-methyl-4-(4-hydroxystyryl)pyridinium cation (HSP^+). The *trans*-HSP^+ structure shows the numbering of the aromatic protons. The irradiation wavelengths typically are: hν >350 nm and hν' <300 nm.

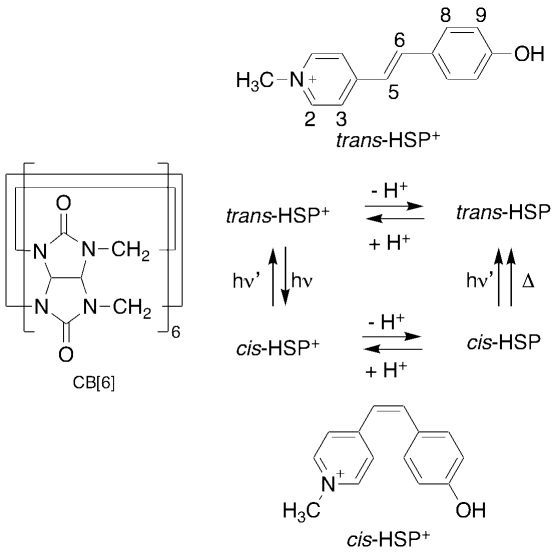

EXPERIMENTAL SECTION

Materials: The synthesis of *trans*-HSP was based on a previous procedure[39] with the quantity of aldehyde reduced, simplifying the purification via crystallization.[40] CB[6] ($C_{24}H_{12}N_{24}O_{12}$) was synthesized according to the literature with some modifications.[41-42] Standardized volumetric solutions of HCl (Anachemia, ACS reagent grade), standardized volumetric solutions of NaOH (Anachemia, ACS reagent grade), methanol (Caledon Laboratories, spectral grade, > 99.8%), NaCl (BDH), D_2O (Cambridge Isotope Laboratories, Inc., 99.9%) and DCl (Cambridge Isotope Laboratories, Inc., 99.5% isotopically pure, 35% in D_2O) were used without further purification. Deionized water (≥17.8 MΩ cm) was prepared on a Barnstead NANOpure deionizing system and was used for all experiments except NMR studies.

Sample preparation: HCl (1.000 M) and NaOH (1.000 M) stock solutions were prepared by dilution, and NaCl stock solutions (2.000 M) were prepared by dissolving the solid in water.

Solutions with lower concentrations of HCl, NaOH and NaCl were prepared by dilution of the respective stock solutions. CB[6] stock solutions (4.00 mM) were prepared by dissolving the solids in 0.1 M NaCl solutions, since binding of Na^+ to CB[6] aids in the solubilization of CB[6]. This concentration of Na^+ ensured that CB[6] was soluble in NaCl/water in the stock solution and for the highest CB[6] concentration used in the experiments (1 mM, $[Na^+] \geq 0.05$ M). Stock solutions of *trans*-HSP (1.00 mM) were prepared by dissolving the solid in methanol where only *trans*-HSP was present, since *cis*-HSP is not stable in methanol.[38] The separate samples of *trans*-HSP and CB[6] were prepared by diluting the respective stock solutions into NaOH (1 mM)/NaCl and HCl (3 mM)/NaCl solutions. The Na^+ cation concentrations were the same for the CB[6] and *trans*-HSP solutions. The presence of 1 mM NaOH in the *trans*-HSP solution ensured that *trans*-HSP was fully deprotonated. *cis*-HSP was not present in this solution since *cis*-HSP would be readily isomerized photochemically and thermally (Scheme 1).[38] Unless otherwise stated, the concentration of HCl in CB[6] solutions (3 mM) was higher than the concentration of NaOH (1mM) in the *trans*-HSP solutions, leading to a final H_3O^+ concentration of 1 mM when equal volumes of these two solutions were mixed. This concentration differential ensures that *trans*-HSP was fully protonated after the mixing of equal volumes of *trans*-HSP/NaOH/NaCl and CB[6]/HCl/NaCl solutions in the stopped-flow experiments. Moreover, the CB[6] and *trans*-HSP solutions were mixed in the dark and were immediately used for UV-Vis and steady-state fluorescence measurements.

For ^1H NMR measurements, DCl solutions were prepared by diluting a 35% DCl/D_2O solution with D_2O. NaCl solutions were prepared by dissolving the solid in D_2O. The *trans*-HSP^+ solution was freshly prepared in the dark by dissolving the *trans*-HSP solid into DCl (2 mM)/NaCl (0.06 M) in D_2O. The *trans*-HSP^+@CB[6] solution was freshly prepared in the dark by dissolving the

CB[6] solid into the *trans*-HSP^+ solution. After measuring the ^1H NMR spectra for *trans*-HSP^+ and *trans*-HSP^+@CB[6] solutions, these samples were irradiated at 368 nm (10 nm bandwidths) for 10 min by placing them in the sample holder of the fluorimeter. The irradiated samples were then used to determine the ^1H NMR spectra for the samples at the photostationary state.

Instruments: A Cary 100 was employed to determine the UV-Vis absorption spectra. A PTI QM-2 fluorimeter was employed to measure the steady-state fluorescence spectra. The excitation wavelength was 374 nm with monochromator bandwidths of 2 nm. The emission spectra were measured from 400 to 700 nm with monochromator bandwidths of 2 nm. The samples were placed in 10 mm × 10 mm quartz cells and equilibrated to 20.0 ± 0.1 °C in the dark for 15 min before the collection of absorption and fluorescence spectra. All spectra were corrected by subtracting the respective baseline spectra, which contained all chemicals except *trans*-HSP^+.

^1H NMR spectra were recorded with a Bruker Avance500 spectrometer (500.1 MHz for ^1H) at room temperature. Proton chemical shifts (δ) are expressed in parts per million (ppm) and are calibrated according to the solvent residual peak (4.79 ppm for DOH).

A SX20 stopped-flow system (Applied Photophysics) was employed to measure the fluorescence changes over time after the mixing of solutions. The samples were excited at a wavelength of 368 nm using a mercury-xenon lamp (Hamamatsu). The dependence of the irradiation beam width on the photoisomerization kinetics was studied using excitation monochromator slit widths ranging from 0.1 to 4 mm. For stopped-flow experiments, the slit bandwidths of the excitation monochromator were set to 0.19 nm or 1.2 nm corresponding to slit widths of 0.04 mm and 0.26 mm, respectively. Fluorescence was collected using a 400 nm cut-off filter (Schott GG 400) placed in front of the detection photomultiplier. The same voltage was used throughout one experiment to ensure that intensities could be compared and the signal intensity

for the fluorescence was lower than 6 V. The *trans*-HSP/NaOH/NaCl and the CB[6]/HCl/NaCl solutions were contained separately in the two injection syringes and were equilibrated at 20.0 ± 0.1 °C for at least 15 min before measurements were performed. A 1:1 mixing ratio was employed. The final concentrations of *trans*-HSP^+ and CB[6] correspond to half of the concentrations of the solutions contained in the syringes. At least 66 kinetic traces were averaged to increase the signal-to-noise ratio. The following control experiments were performed: (i) Injection of water against water to determine the zero intensity value for the system to be subtracted from intensity values for solutions containing *trans*-HSP^+ but not CB[6]; (ii) injection of CB[6] against water to determine the baseline value to be subtracted from all intensities measured for solutions containing CB[6]; (iii) injection of *trans*-HSP^+ against water to determine the emission intensity of *trans*-HSP^+ in the absence of CB[6]. The values for controls (i) and (ii) are very similar and are less than 4% of the emission intensities measured for 2.5 μM *trans*-HSP^+ in experiments (iii) when the monochromator bandwidth was set to 0.19 nm (0.04 mm). The concentrations of HCl, NaOH and NaCl for the control experiments were the same as those for the kinetic experiments for the *trans*-HSP^+@CB[6] complex formation.

The kinetic data from stopped-flow experiments determined in the range of 0.25–150 s or within the first 50 ms were respectively fit with an exponential decay (eq 1) or with an exponential growth (eq 2):

$$I = a_{iso} \times e^{-k_{iso}t} + I_{\infty} + I_w \quad (1)$$

where a_{iso}, k_{iso}, I_∞ and I_w represent the amplitude, the isomerization rate constant, the fluorescence intensity of the solutions at the photostationary state, and the fluorescence intensity of the baseline solutions, respectively.

$$I = I_0 + a_{obs}(1 - e^{-k_{obs}t}) \quad (2)$$

where a_{obs}, k_{obs} and I_0 represent the amplitude, the observed rate constant for the fluorescence change, and the fluorescence intensity at time 0, respectively.

RESULTS and DISCUSSION

The binding of *trans*-HSP$^+$ to CB[6] led to changes in the absorption (Figure S1), fluorescence (Figure S1), and ^{1}H NMR spectra for *trans*-HSP$^+$ (Figure 1). All peaks in the ^{1}H NMR spectrum for *trans*-HSP$^+$ or for the mixture of *cis*- and *trans*-HSP$^+$ at the photostationary state are sharp in the absence of CB[6] (Figure 1a, b). The binding of *trans*-HSP$^+$ to CB[6] led to peak broadening (Figure 1c) that is indicative of slow exchange on the NMR time scale between free and CB[6]-bound *trans*-HSP$^+$. The peaks associated with the hydroxybenzene moiety exhibit the smallest peak broadening, which suggests that this moiety protrudes from CB[6], while the methylpyridinium moiety is encapsulated by the CB[6] cavity. The ^{1}H NMR spectrum for a mixture of both HSP$^+$ isomers and CB[6] shows sharp peaks for *cis*-HSP$^+$ with their positions unchanged by the addition of CB[6], whereas the peaks for *trans*-HSP$^+$ are broadened (Figure 1d); this observation indicates that CB[6] does not form a complex with *cis*-HSP$^+$.

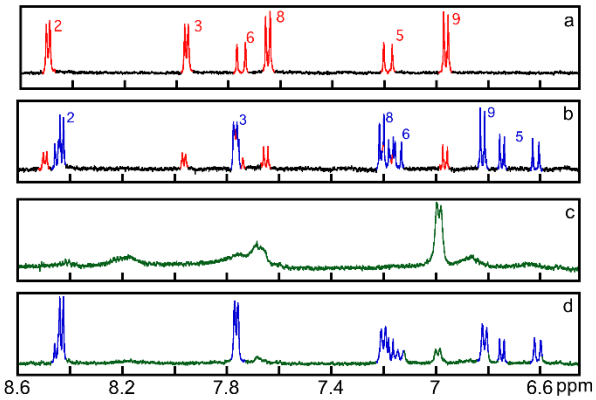

Figure 1. Aromatic region of the ^{1}H NMR spectra for (a) *trans*-HSP^{+} (see Scheme 1 for assignments), (b) *trans*- and *cis*-HSP^{+} at the photostationary state (λ_{ex} = 368 nm), (c) *trans*-HSP^{+} and CB[6], and (d) *trans*-HSP^{+}, *cis*-HSP^{+}, and CB[6]. [HSP^{+}]$_{total}$ = 0.25 mM, [DCl] = 2 mM, and [NaCl] = 0.06 M for all spectra, and CB[6] = 0.5 mM for spectra c and d. The signals for *trans*-HSP^{+}, *cis*-HSP^{+}, and *trans*-HSP^{+}@CB[6] are labeled respectively in red, blue, and green.

The kinetics was studied by stopped flow using fluorescence detection with samples under continuous irradiation after fast mixing (≤1 ms). The designed pH jump experiment minimized the photoisomerization of *trans*-HSP^{+} other than during the experiment, because the guest solution of *trans*-HSP prepared in 1 mM NaOH ensures that all HSP molecules are in the stable deprotonated *trans* form before mixing occurs. The CB[6] solution was prepared in 3 mM HCl. When the two solutions are mixed in the stopped flow, resulting in a final hydronium ion (H_3O^{+}) concentration of 1 mM, the protonation of *trans*-HSP happens instantaneously within the mixing time of the experiment. Therefore, the formation of *trans*-HSP^{+} can be considered as a pre-equilibrium process that was complete before the onset of *trans*-to-*cis* isomerization and host–guest complexation. NaCl was added to enhance the CB[6] solubility[43-47] by binding cations to the CB[6]

portals. The concentration of H_3O^+ used is sufficiently low to ensure that less than 0.1% of CB[6] is bound to H_3O^+ but high enough to protonate all *trans*-HSP (pK_a = 8.57,[48] Table S1).

The *trans*-to-*cis* photoisomerization depends on the photon flux, whereas the binding kinetics of *trans*-HSP^+ to CB[6] is independent of this flux. The photoisomerization rate was controlled by the width of the irradiation beam used for fluorescence detection on the stopped-flow apparatus (Figure S2). No photoisomerization occurred with a beam width of 0.1 mm, whereas the maximum rate was achieved with a beam width of 3 mm or wider, reaching the photostationary state within 10 s. The formation of the *trans*-HSP^+@CB[6] complex occurred on a faster time scale (≤50 ms) with a rate that was at least 200 times faster than the photoisomerization rate. Therefore, the two processes are temporally uncoupled.

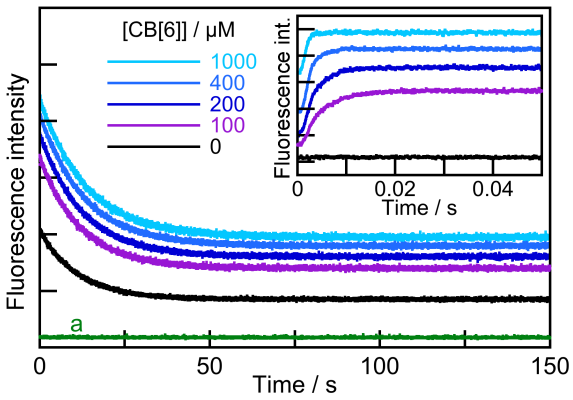

Figure 2. Kinetics for the mixing of *trans*-HSP/NaOH/NaCl with CB[6]/HCl/NaCl solutions ($[trans\text{-}HSP^+]_{final}$ = 2.5 μM, $[H_3O^+]_{final}$ = 1 mM, $[Na^+]$ = 0.05 M, λ_{ex} = 368 nm, irradiation beam width of 0.26 mm). Trace "a" (green) corresponds to the baseline of NaOH/NaCl mixed with HCl/NaCl. Inset: Kinetics over the first 50 ms. The CB[6] concentrations indicated are final ones.

At the excitation wavelength of 368 nm used for the stopped-flow experiments, the molar absorptivity of *trans*-HSP$^+$ is higher than for *cis*-HSP$^+$,[38] leading to a decrease of the emission intensity when *cis*-HSP$^+$ is formed (Figure 2). In contrast, complexation of *trans*-HSP$^+$ to CB[6] leads to an increase in the emission intensity (inset Figure 2, Figure S1). Therefore, the growth kinetics for HSP$^+$@CB[6] formation is followed by the decay kinetics for the photoisomerization (Figure 2). The kinetics for *trans*-HSP$^+$ photoisomerization and HSP$^+$@CB[6] complex formation can be analyzed separately because of the temporal uncoupling of these two processes.

The decays for the photoisomerization reaction fit adequately to a monoexponential function (eq 1, Figure S3) between 0.25 and 150 s, indicating that photoisomerization occurred through a single relaxation process. The observed rate constant (k_{iso}) for the photoisomerization reaction decreased from 0.0895 ± 0.0002 s^{-1} in the absence of CB[6] to 0.0731 ± 0.0002 s^{-1} in the presence of 1 mM CB[6], showing that the formation of *trans*-HSP$^+$@CB[6] slows the *trans*-to-*cis* photoisomerization (Table S2).

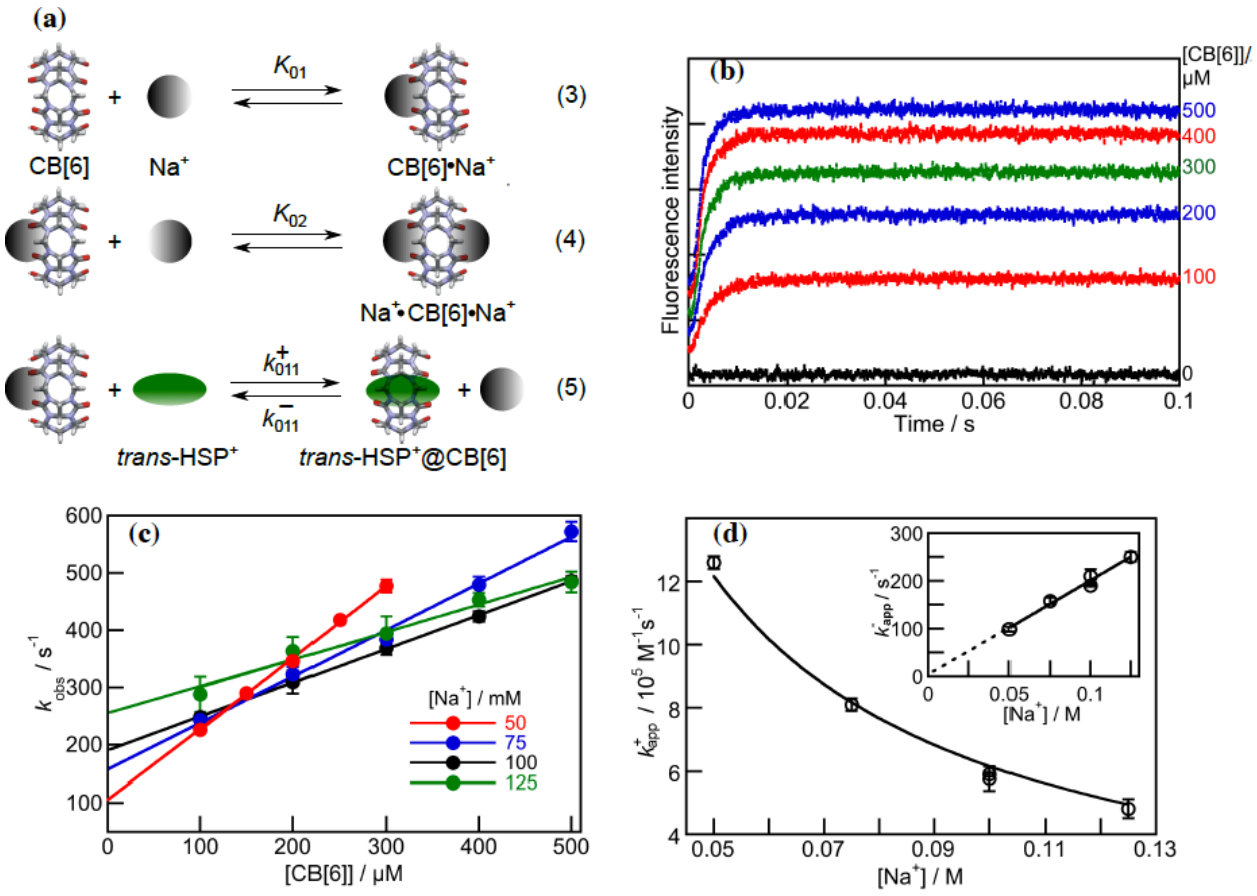

Figure 3. (a) *trans*-HSP$^+$/CB[6]/Na$^+$ binding mechanism expressed by equations 3 to 5, where "•" and "@" represent binding to the CB[6] portals (exclusion complex) and in the CB[6] cavity (inclusion complex), respectively. (b) Kinetics for the mixing of *trans*-HSP/NaOH/NaCl with CB[6]/HCl/NaCl solutions ([*trans*-HSP$^+$]$_{final}$ = 2.5 μM, [H_3O^+]$_{final}$ = 1 mM, [Na$^+$] = 0.1 M, irradiation beam width of 0.04 mm). (c) Dependence of k_{obs} on the CB[6] concentration (eq 6) for the mixing of *trans*-HSP/NaOH/NaCl with CB[6]/HCl/NaCl at different Na$^+$ ion concentrations ([*trans*-HSP$^+$]$_{final}$ = 2.5 μM, [H_3O^+]$_{final}$ = 1 mM, irradiation beam width of 0.04 mm). The error bars correspond to standard deviations (≥3 independent experiments); nonvisible error bars are smaller than the data points. (d) Dependence of k_{app}^{+} on the Na$^+$ concentration. The black line corresponds to the fit of the data to eq 8 with K_{02} = 780 M^{-1}. Inset: Dependence of k_{app}^{-} on the

Na^+ concentration. The solid black line corresponds to the fit of the data to eq 7, whereas the dashed line is the extrapolation of this fit.

The kinetics for *trans*-HSP^+@CB[6] formation became faster and the amplitude for the kinetics was larger at higher CB[6] concentrations (inset, Figure 2), consistent with a bimolecular reaction. These kinetic studies are consistent with a mechanism (Figure 3a, eq. 3-5) where Na^+ cations bind sequentially to CB[6], as previously shown for a CB[7] complex,[29] and *trans*-HSP^+ binds with CB[6]•Na^+ releasing the Na^+ cation. The kinetics data (Figure 3b) fit well to a monoexponential function (eq 2, Figure S4), showing that one relaxation process occurs for the formation of the complex. Na^+ cation binding to CB[6] is in fast equilibrium and the concentration ratios for CB[6], CB[6]•Na^+, and Na^+•CB[6]•Na^+ are constant throughout the kinetics. The observed rate constants (k_{obs}) depend linearly on the CB[6] concentration (eq 6, Figure 3c). The apparent association (k_{app}^{+}) and dissociation (k_{app}^{-}) rate constants (eqs 7 and 8) depend on the Na^+ cation concentration (see derivations in the SI and eq S31).

$$k_{obs} = k_{app}^{+}\left[\mathrm{CB[6]}\right]_{\mathrm{T}} + k_{app}^{-} \tag{6}$$

$$k_{app}^{-} = k_{011}^{-}[\mathrm{Na^+}] \tag{7}$$

$$k_{app}^{+} = \frac{k_{011}^{+}}{1 + K_{02}[\mathrm{Na^+}]} \tag{8}$$

The concentration of free CB[6] is negligible (Table S1) and no binding of *trans*-HSP^+ to free CB[6] occurs for the Na^+ cation concentrations used (50–125 mM). All the kinetic traces are monoexponential and k_{obs} depends linearly on the CB[6] concentration (Figure 3c). Thus, the only host species available to bind *trans*-HSP^+ is CB[6]•Na^+, as Na^+•CB[6]•Na^+ does not bind the guest.

The key observation supporting the binding of the guest to CB[6]•Na^+ is the increase of the intercept, which corresponds to k_{app}^-, with the Na^+ ion concentration (Figure 3c). This increase is consistent with a dissociation process that involves Na^+ in a bimolecular reaction. In contrast, k_{app}^+ decreases (slope in eq 6, Figure 3c) as the Na^+ cation concentration increases because CB[6] is occupied as Na^+•CB[6]•Na^+. Thus, Na^+ cations play opposing roles in the association and dissociation dynamics of *trans*-HSP^+@CB[6].

The dissociation of *trans*-HSP^+ from *trans*-HSP^+@CB[6] could potentially also occur through a unimolecular process (k_{001}^-) without the participation of the Na^+ cation (eq 9, Scheme S2). The binding of the guest solely to free CB[6] is inconsistent with the results, as in that case, k_{app}^- would not depend on the Na^+ cation concentration.[29] The value for the unimolecular dissociation rate constant without Na^+ participation (k_{001}^-) is 3 ± 15 s^{-1} (inset, Figure 3d), while the rate constant for the bimolecular reaction with Na^+ (k_{011}^-) is (2.0 ± 0.2) × 10^3 M^{-1} s^{-1}. The value for the unimolecular dissociation rate constant is small and suggests a negligible contribution from this Na^+-independent reaction considering the Na^+ concentrations used. Therefore, equation 9 can be simplified to eq 7.

$$k_{app}^- = k_{001}^- + k_{011}^-[Na^+] \quad (9)$$

The association rate constant of HSP^+ with CB•Na^+ (k_{011}^+) is (4.87 ± 0.09) × 10^7 M^{-1} s^{-1} (eq 8, Figure 3d), with an assumed K_{02} value of 780 M^{-1}. This K_{02} value corresponds to 25% of the K_{01} value (3.1 × 10^3 M^{-1}),[49] and is, on statistical grounds,[50] the upper limit for K_{02}. Varying the assumed K_{02} value (Figure S5) gave adequate fits for values between 310 and 780 M^{-1}, leading to an uncertainty of a factor of 2.5 for k_{011}^+ (Table S3). For the remainder of the analysis, the upper limit

for K_{02} was assumed based on previous studies where the binding constant for the second Na^+ cation to CB[7] was shown to be close to its upper theoretical limit.[29]

The equilibrium constant for the formation of *trans*-HSP^+@CB[6] (eq 5, Figure 3a) corresponds to the ratio of the rate constants for the bimolecular association (k_{011}^{+}) and dissociation (k_{011}^{-}) reactions. This calculated equilibrium constant is $(2.4 \pm 0.3) \times 10^4$.

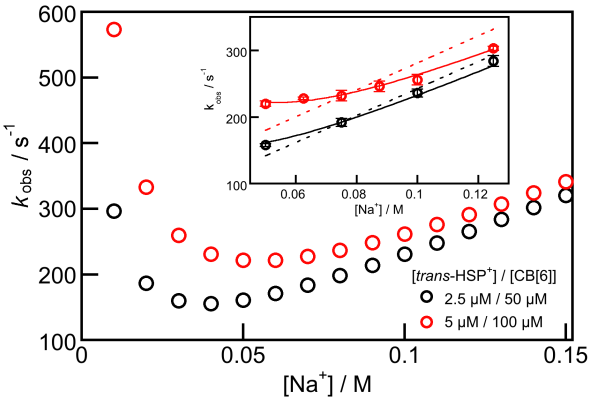

Figure 4. Dependence of calculated k_{obs} on the Na^+ concentration (eqs 6–8, K_{02} = 780 M^{-1}, k_{011}^{+} = 4.87 × 10^7 M^{-1} s^{-1}, k_{011}^{-} = 2.0 × 10^3 M^{-1} s^{-1}). Inset: Dependence of experimental k_{obs} on the Na^+ concentration at a constant [CB[6]]/[*trans*-HSP^+] ratio of 20 when mixing *trans*-HSP/NaOH/NaCl with CB[6]/HCl/NaCl solutions. The solid lines correspond to the fits of the data using eqs 6–8 with the above-mentioned parameter values. The dashed line corresponds to the fit of the data for the binding of only one Na^+ to CB[6] (eq S79).

The binding of one or two metal cations to CB[*n*]s is an ongoing mechanistic question.[3, 29, 51-53] If CB[6] binds only one Na^+, a linear relationship is expected between k_{obs} and the Na^+ cation concentration (eq S79), which disagrees with the results (inset, Figure 4 and Figures S6 and S7 for fits at the higher HSP^+ and CB[6] concentrations). The nonlinear behavior of k_{obs} with the Na^+

cation concentration (Figure 4) reflects the opposing effects of this cation on the apparent association (k_{app}^{+}, eq 8) and dissociation (k_{app}^{-}, eq 7) rate constants. This nonlinearity is a consequence of the sequential binding of Na^+ to CB[6] to form CB[6]•Na^+, which binds the guest, whereas Na^+•CB[6]•Na^+ does not bind a guest and suppresses the association rate. At low Na^+ cation concentrations, k_{obs} increases because the relative concentration of Na^+•CB[6]•Na^+ is low. In contrast, at high Na^+ cation concentrations, k_{obs} is predominantly determined by the dissociation process, leading to a linear dependence of k_{obs} on the Na^+ cation concentration (Figure 4). The nonlinearity is less pronounced when lower *trans*-HSP^+ and CB[6] concentrations are used and for Na^+ concentrations above 70 mM. This dependence on the relative concentrations of guest, host, and metal cation may explain why the binding of only one metal cation to CB[*n*]s has been proposed in some studies.

No unifying mechanism for guest binding to CB[*n*]s exists. Metal cations can have a passive role in modulating the concentration of CB[*n*] that can bind the guest or an active role by interacting directly with the guest–CB[*n*] complex. In the latter role, metal cations can enhance the binding dynamics by speeding up the dissociation or association processes,[32, 54] or the cation can slow down the binding dynamics by forming ternary complexes where the metal cation caps the complex (guest@CB[*n*]•metal cation).[32] Comparisons between studies are difficult because the effect of metal cations has not always been studied (see SI for a reanalysis of data and mechanistic comparisons). The *trans*-HSP^+–CB[6] system has a similar mechanism to the binding of 4-methylbenzylammonium to CB[6], where in the presence of K^+, a nonlinear dependence on the metal cation was observed.[55] In the case of cyclohexylmethylammonium cation[56] and 4-amino-4′-nitroazobenzene[57] binding to CB[6], a ternary complex was formed in the presence of Na^+ and H_3O^+, respectively. A reanalysis of the previous data[56-57] (Figures S8 and S9) showed that the

association rate constant for *trans*-HSP$^+$ with CB[6] is at least 100 times higher than those for these other guests. A direct comparison of the k_{011}^- values to the dissociation rate constants for other reported systems is not possible because, unlike the unimolecular dissociations reported elsewhere,[56-58] the dissociation for *trans*-HSP$^+$@CB[6] is a bimolecular process. Nevertheless, the apparent dissociation rate constant (k_{app}^-), which ranged from 100 to 250 s^{-1} for Na^+ cation concentrations between 50 and 125 mM, is significantly higher than the unimolecular dissociation rate constants for other guest–CB[6] systems in aqueous solution.[56-58] The comparisons of the different guest–CB[6] systems shows that the binding dynamics of guests with CB[6] can occur over different time domains and by different types of mechanisms.

The original objective of this work, which was to study the coupling of the complexation kinetics with a photochemical reaction, could not be achieved because of the slow photoisomerization rate. However, the nonlinear effect of Na^+ on the guest complexation kinetics with CB[*n*]s can in future be explored to change the rate-limiting step of coupled reactions between complex formation and a second reaction of interest for the CB[*n*]-bound guest. At low and high metal cation concentrations, guest complexation is fast and the reaction of interest will be rate limiting. However, at intermediate metal cation concentrations, corresponding to the minimum in Figure 4, the rate of complexation could become rate limiting, potentially changing the outcome of competitive reactions. The results of this study show that by exploring the nonlinearity of the kinetic behavior for a guest–CB[*n*]–metal cation system with the concentration of one of the components, the mechanistic outcome of the system can be controlled. This type of control is the ultimate goal in the development of functional supramolecular systems.

CONCLUSIONS

A guest–CB[6] system was designed to study the kinetics of complex formation in the presence of a competitive reaction for the guest that could be initiated on demand. Photoisomerization of *trans*-HSP^+ was slower than the formation of *trans*-HSP^+@CB[6], and these reactions are temporally uncoupled. *trans*-HSP^+, but not *cis*-HSP^+, binds to CB[6]•Na^+ with the release of the cation. Na^+ cations have an opposing effect on the association and dissociation rates leading to the nonlinear dependence of the observed rate constant on the Na^+ concentration. This nonlinearity depends on the concentration ratio of the systems components, *trans*-HSP^+, CB[6], and Na^+, and linear dependencies with the metal cation concentration can be obtained over narrow concentration ranges for the system's components. The nonlinear dependence observed provides a framework to control the reactivity of systems where guest–CB[6] complex formation is coupled with a reaction of the guest either in the aqueous solution or within the complex.

ASSOCIATED CONTENT

Supporting Information. Absorption and steady-state fluorescence studies, details of stopped-flow kinetics measurements, reanalysis of previously reported guest@CB[6] complexes, and derivations of the observed rate constants for different host–guest binding models (PDF file).

AUTHOR INFORMATION

Corresponding Author

*Email: cornelia.bohne@gmail.com

*Email: kkim@postech.ac.kr

*Email: jnwilson@miami.edu

Present Addresses

[#] H.T.: School of Chemistry and Chemical Engineering, South China University of Technology, 381 Wushan Road, Guangzhou 510641, China

[&] P.N.: Department of Chemistry and Centre for Advanced Studies in Chemistry, Panjab University, Chandigarh 160014, India

Notes

The authors declare no competing financial interests.

ACKNOWLEDGMENT

The authors at the University of Victoria thank the Natural Sciences and Engineering Research Council of Canada (NSERC) for financial support (RGPIN-121389-2012, RGPIN-2017-04458) and CAMTEC for the use of shared facilities. This work was also supported by the Institute for Basic Science (IBS) (IBS-R007-D1) (KK).

REFERENCES

1. Cao, L.; Šekutor, M.; Zavalij, P. Y.; Mlinarić-Majerski, K.; Glaser, R.; Isaacs, L. Cucurbit[7]uril·Guest Pair with an Attomolar Dissociation Constant. *Angew. Chem. Int. Ed.* **2014,** *53*, 988-993.
2. Dsouza, R. N.; Hennig, A.; Nau, W. M. Supramolecular Tandem Enzyme Assays. *Chem. Eur. J.* **2012,** *18*, 3444-3459.
3. Rekharsky, M. V.; Mori, T.; Yang, C.; Ko, Y. H.; Selvapalam, N.; Kim, H.; Sobransingh, D.; Kaifer, A. E.; Liu, S.; Isaacs, L. et.al. A Synthetic Host-guest System Achieves Avidin-biotin Affinity by Overcoming Enthalpy– entropy Compensation. *Proc. Natl. Acad. Sci. U. S. A* **2007,** *104*, 20737-20742.
4. Shetty, D.; Khedakar, J. K.; Park, K. M.; Kim, K. Can we Beat the Biotin–avidin Pair?: Cucurbit[7]uril-based Ultrahigh Affinity Host–guest Complexes and their Applications. *Chem. Soc. Rev.* **2015,** *44*, 8747-8761.

5. Lazar, A. I.; Rohacova, J.; Nau, W. M. Comparison of Complexation-Induced pK_a Shifts in the Ground and Excited States of Dyes as Well as Different Macrocyclic Hosts and Their Manifestation in Host-Retarded Excited-Dye Deprotonation. *J. Phys. Chem. B* **2017,** *121*, 11390-11398.
6. Macartney, D. H. Cucurbit[n]uril Host-Guest Complexes of Acids, Photoacids, and Super Photoacids. *Isr. J. Chem.* **2018,** *58*, 230-243.
7. Mock, W. L.; Pierpont, J. A Cucurbituril-Based Molecular Switch. *J. Chem. Soc. Chem. Commun.* **1990**, 1509-1511.
8. Saleh, N.; Koner, A. L.; Nau, W. M. Activation and Stabilization of Drugs by Supramolecular pK_a Shifts: Drug-delivery Applications Tailored for Cucurbiturils. *Angew. Chem., Int. Ed.* **2008,** *47*, 5398-5401.
9. Basílio, N.; Gago, S.; Parola, A. J.; Pina, F. Contrasting pK_a Shifts in Cucurbit[7]uril Host−Guest Complexes Governed by an Interplay of Hydrophobic Effects and Electrostatic Interactions. *ACS Omega* **2017,** *2*, 70-75.
10. Ong, W.; Kaifer, A. E. Unusual Electrochemical Properties of the Inclusion Complexes of Ferrocenium and Cobaltocenium with Cucurbit[7]uril. *Organometallics* **2003,** *22*, 4181-4183.
11. Zheng, Y.; Kaifer, A. E. Ternary Complex Formation by Cucurbit[7]uril Leads to Large Shifts in the Reduction Potentials of Suitable Viologens. *ChemElectroChem* **2019,** *6*, 5610-5616.
12. Barrow, S. J.; Kasera, S.; Rowland, M. J.; del Barrio, J.; Scherman, O. A. Cucurbituril-Based Molecular Recognition. *Chem. Rev.* **2015,** *115*, 12320-12406.
13. Cera, L.; Schalley, C. A. Stimuli-induced Folding Cascade of a Linear Oligomeric Guest Chain Programmed through Cucurbit[n]uril Self-sorting (n = 6, 7, 8). *Chem. Sci.* **2014,** *5*, 2560-2567.
14. Kotturi, K.; Masson, E. Directional Self-Sorting with Cucurbit[8]uril Controlled by Allosteric π–π and Metal–Metal Interactions. *Chem. Eur. J.* **2018,** *24*, 8670-8678.
15. Liu, S.; Ruspic, C.; Mukhopadhyay, P.; Chakrabarti, S.; Zavalij, P. Y.; Isaacs, L. The Cucurbit[n]uril Family: Prime Components for Self-Sorting Systems. *J. Am. Chem. Soc.* **2005,** *127*, 15959-15967.
16. Mukhopadhyay, P.; Zavalij, P. Y.; Isaacs, L. High Fidelity Kinetic Self-Sorting in Multi-Component Systems Based on Guests with Multiple Binding Epitopes. *J. Am. Chem. Soc.* **2006,** *128*, 14093-14102.
17. Barbero, H.; Thompson, N. A.; Masson, E. "Dual Layer" Self-Sorting with Cucurbiturils. *J. Am. Chem Soc.* **2020,** *142*, 867-873.
18. Li, Q.-L.; Sun, Y.; Sun, Y.-L.; Wen, J.; Zhou, Y.; Bing, Q.-M.; Isaacs, L. D.; Jin, Y.; Gao, H.; Yang, Y.-W. Mesoporous Silica Nanoparticles Coated by Layer-by-Layer Self-assembly Using Cucurbit[7]uril for in Vitro and in Vivo Anticancer Drug Release. *Chem. Mater.* **2014,** *26*, 6418-6431.
19. Robinson-Duggon, J.; Pérez-Mora, F.; Dibona-Villanueva, L.; Fuentealba, D. Potential Applications of Cucurbit[n]urils Inclusion Complexes in Photodynamic Therapy. *Isr. J. Chem.* **2018,** *58*, 199-214.
20. Samanta, S. K.; Moncelet, D.; Briken, V.; Isaacs, L. Metal–Organic Polyhedron Capped with Cucurbit[8]uril Delivers Doxorubicin to Cancer Cells. *J. Am. Chem. Soc.* **2016,** *138*, 14488-14496.
21. Walker, S.; Oun, R.; McInnes, F. J.; Wheate, N. J. The Potential of Cucurbit[n]urils in Drug Delivery. *Isr. J. Chem.* **2011,** *51*, 616-624.

22. Das, D.; Assaf, K. I.; Nau, W. M. Applications of Cucurbiturils in Medicinal Chemistry and Chemical Biology. *Front. Chem.* **2019,** *7:*619.
23. Zou, L.; Braegelman, A. S.; Webber, M. J. Spatially Defined Drug Targeting by in Situ Host−Guest Chemistry in a Living Animal. *ACS Cent. Sci.* **2019,** *5*, 1035-1043.
24. Remón, P.; González, D.; Romero, M. A.; Basílio, N.; Pischel, U. Chemical Signal Cascading in a Supramolecular Network. *Chem. Commun.* **2020,** *56*, 3737-3740.
25. Ghale, G.; Nau, W. M. Dynamically Analyte-Responsive Macrocyclic Host−Fluorophore Systems. *Acc. Chem. Res.* **2014,** *47*, 2150-2159.
26. Liu, Y.-C.; Peng, S.; Angelova, L.; Nau, W. M.; Hennig, A. Label-Free Fluorescent Kinase and Phosphatase Enzyme Assays with Supramolecular Host-Dye Pairs. *ChemistryOpen* **2019,** *8*, 1350-1354.
27. Liu, Y.-C.; Nau, W. M.; Hennig, A. A Supramolecular Five-component Relay Switch that Exposes the Mechanistic Competition of Dissociative versus Associative Binding to Cucurbiturils by Ratiometric Fluorescence Monitoring. *Chem. Commun.* **2019,** *55*, 14123-14126.
28. Xu, W.; Song, Q.; Xu, J.-F.; Serpe, M. J.; Zhang, X. Supramolecular Hydrogels Fabricated from Supramonomers: A Novel Wound Dressing Material. *ACS Appl. Mater. Interfaces* **2017,** *9*, 11368-11372.
29. Tang, H.; Fuentealba, D.; Ko, Y. H.; Selvapalam, N.; Kim, K.; Bohne, C. Guest Binding Dynamics with Cucurbit[7]uril in the Presence of Cations. *J. Am. Chem. Soc.* **2011,** *133*, 20623-20633.
30. Ong, W.; Kaifer, A. E. Salt Effects on the Apparent Stability of the Cucurbit[7]uril-Methyl Viologen Inclusion Complex. *J. Org. Chem.* **2004,** *69*, 1383-1385.
31. Shinde, M. N.; Choudhury, S. D.; Barooah, N.; Pal, H.; Bhasikuttan, A. C.; Mohanty, J. Metal-Ion-Mediated Assemblies of Thiazole Orange with Cucurbit[7]uril: A Photophysical Study. *J. Phys. Chem. B* **2015,** *119*, 3815-3823.
32. Thomas, S. S.; Tang, H.; Bohne, C. Noninnocent Role of Na^+ Ions in the Binding of the N-Phenyl-2-naphthylammonium Cation as a Ditopic Guest with Cucurbit[7]uril. *J. Am. Chem Soc.* **2019,** *141*, 9645-9654.
33. Mock, W. L.; Irra, T. A.; Wepsiec, J. P.; Adhya, M. Catalysis by Cucurbituril. The Significance of Bound-Substrate Destabilization for Induced Triazole Formation. *J. Org. Chem.* **1989,** *54*, 5302-5308.
34. Vallavoju, N.; Sivaguru, J. Supramolecular Photocatalysis: Combining Confinement and Non-covalent Interactions to Control Light Initiated Reactions. *Chem. Soc. Rev.* **2014,** *43*, 4084-4101.
35. Assaf, K. I.; Nau, W. M. Cucurbiturils: from Synthesis to High-affinity Binding and Catalysis. *Chem. Soc. Rev.* **2015,** *44*, 394-418.
36. Palma, A.; Artelsmair, M.; Wu, G.; Lu, X.; Barrow, S. J.; Uddin, N.; Rosta, E.; Masson, E.; Scherman, O. A. Cucurbit[7]uril as a Supramolecular Artificial Enzyme for Diels–Alder Reactions. *Angew. Chem., Int. Ed.* **2017,** *56*, 15688-15692.
37. Masson, E.; Raeisi, M.; Kotturi, K. Kinetics Inside, Outside and Through Cucurbiturils. *Isr. J. Chem.* **2018,** *58*, 413-434.
38. Steiner, U.; Abdel-Kader, M. H.; Fischer, P.; Kramer, H. E. A. Photochemical cis/trans Isomerization of a Stilbazolium Betaine. A Protolytic/photochemical Reaction Cycle. *J. Am. Chem. Soc.* **1978,** *100*, 3190-3197.
39. Phillips, A. P. Condensation of Aromatic Aldehydes with γ-Picoline Methiodide. *J. Org. Chem.* **1949,** *14*, 302-305.

40. Brown, A. S.; Bernal, L.-M.; Micotto, T. L.; Smith, E. L.; Wilson, J. N. Fluorescent Neuroactive Probes Based on Stilbazolium Dyes. *Org. Biomol. Chem.* **2011,** *9*, 2142-2148.
41. Freeman, W. A.; Mock, W. L.; Shih, N. Y. Cucurbituril. *J. Am. Chem. Soc.* **1981,** *103*, 7367-7368.
42. Lim, S.; Kim, H.; Selvapalam, N.; Kim, K.-J.; June Cho, S.; Seo, J. G.; Kim, K. Cucurbit[6]uril: Organic Molecular Porous Material with Permanent Porosity, Exceptional Stability, and Acetylene Sorption Properties. *Angew. Chem. Int. Ed.* **2008,** *47*, 3352-3355.
43. Buschmann, H.-J.; Cleve, E.; Schollmeyer, E. Cucurbituril as a Ligand for the Complexation of Cations in Aqueous Solutions. *Inorg. Chim. Acta* **1992,** *193*, 93-97.
44. Buschmann, H. J.; Jansen, K.; Meschke, C.; Schollmeyer, E. Thermodynamic Data for Complex Formation between Cucurbituril and Alkali and Alkaline Earth Cations in Aqueous Formic Acid Solution. *J. Solution Chem.* **1998,** *27*, 135-140.
45. Jeon, Y.-M.; Kim, J.; Whang, D.; Kim, K. Molecular Container Assembly Capable of Controlling Binding and Release of Its Guest Molecules: Reversible Encapsulation of Organic Molecules in Sodium Ion Complexed Cucurbituril. *J. Am. Chem. Soc.* **1996,** *118*, 9790-9791.
46. Jansen, K.; Buschmann, H. J.; Wego, A.; Döpp, D.; Mayer, C.; Drexler, H. J.; Holdt, H. J.; Schollmeyer, E. Cucurbit[5]uril, Decamethylcucurbit[5]uril and Cucurbit[6]uril. Synthesis, Solubility and Amine Complex Formation. *J. Inclusion Phenom. Macrocyclic Chem.* **2001,** *39*, 357-363.
47. Whang, D.; Park, K.-M.; Heo, J.; Ashton, P.; Kim, K. Molecular Necklace: Quantitative Self-Assembly of a Cyclic Oligorotaxane from Nine Molecules. *J. Am. Chem. Soc.* **1998,** *120*, 4899-4900.
48. Kuder, J. E.; Wychick, D. Acid-base Equilibria in the Ground and Excited States of a Solvatochromic Merocyanine Dye. *Chem. Phys. Letters* **1974,** *24*, 69-72.
49. Buschmann, H. J.; Cleve, E.; Jansen, K.; Wego, A.; Schollmeyer, E. Complex Formation between Cucurbit[n]urils and Alkali, Alkaline Earth and Ammonium Ions in Aqueous Solution. *J. Incl. Phenom. Macrocyclic Chem.* **2001,** *40*, 117-120.
50. Connors, K. A. *Binding Constants - The Measurement of Molecular Complex Stability*. John Wiley & Sons: New York, 1987.
51. Megyesi, M.; Biczók, L.; Jablonkai, I. Highly Sensitive Fluorescence Response to Inclusion Complex Formation of Berberine Alkaloid with Cucurbit[7]uril. *J. Phys. Chem. C* **2008,** *112*, 3410-3416.
52. Shaikh, M.; Mohanty, J.; Bhasikuttan, A. C.; Uzunova, V. D.; Nau, W. M.; Pal, H. Salt-induced Guest Relocation from a Macrocyclic Cavity into a Biomolecular Pocket: Interplay between Cucurbit[7]uril and Albumin. *Chem. Commun.* **2008**, 3681-3683.
53. Zhang, S.; Grimm, L.; Miskolczy, Z.; Biczók, L.; Frank Biedermann, F.; Nau, W. M. Binding Affinities of Cucurbit[n]urils with Cations. *Chem. Commun.* **2020,** *55*, 14131-14134.
54. Miskolczy, Z.; Megyesi, M.; Biczók, L.; Prabodh, A.; Biedermann, F. Kinetics and Mechanism of Cation-induced Guest Release from Cucurbit[7]uril. *Chem. Eur. J.* **2020**, *26*, 7433-7441.
55. Hoffmann, R.; Knoche, W.; Fenn, C.; Buschmann, H.-J. Host–guest Complexes of Cucurbituril with the 4-Methylbenzylammonium lon, Alkali-metal Cations and NH_4^+. *J. Chem. Soc., Faraday Trans.* **1994,** *90*, 1507-1511.
56. Márquez, C.; Hudgins, R. R.; Nau, W. M. Mechanism of Host-Guest Complexation by Cucurbituril. *J. Am. Chem. Soc.* **2004,** *126*, 5806-5816.

57. Neugebauer, R.; Knoche, W. Host-guest Complexes of Cucurbituril with 4-Amino-4'-nitroazobenzene and 4,4'-Diaminoazobenzene in Acidic Aqueous Solutions. *J. Chem. Soc., Perkin Trans. 2* **1998**, 529-534.
58. Mock, W. L.; Shih, N. Y. Structure and Selectivity in Host-Guest Complexes of Cucurbituril. *J. Org. Chem.* **1986,** *51*, 4440-4446.

TOC Graphic